



Zurich University of Applied Sciences

Department Life Sciences and Facility Management

Institute of Natural Resource Sciences

TERM PAPER 1

ecoacoustics

Author:

Julian Kraft¹

Tutor:

Dr. Matthias Nyfeler²

Affiliations:

¹Institute of Natural Resource Sciences

²Institute of Computational Life Sciences

Imprint

Project type: Term Paper 1
Title: ecoacoustics
Date: June 30, 2024
Keywords: ecoacoustics, bioacoustics, classification, deeplearning, machinelearning, signalprocessing, audioanalysis
Copyright: Zurich University of Applied Sciences

Author: Julian Kraft¹ (kraftjul@students.zhaw.ch)
Tutor: Dr. Matthias Nyfeler² (nife@zhaw.ch)
Affiliations: ¹Institute of Natural Resource Sciences
²Institute of Computational Life Sciences

Abstract

Contents

| | |
|--|-----------|
| 1. Introduction | 1 |
| 1.1. Background | 1 |
| 2. Methods | 3 |
| 2.1. Dataset | 3 |
| 2.2. Programming Language and Frameworks | 3 |
| 2.3. Deep Learning Model | 3 |
| 2.4. Data Processing | 4 |
| 2.4.1. Sampling | 4 |
| 2.4.2. Transformation | 5 |
| 2.5. Fitting the Model | 6 |
| 2.5.1. Training | 6 |
| 2.5.2. Hyperparameter Tuning | 6 |
| 2.6. Evaluation | 7 |
| 2.6.1. Metrics and Tests | 7 |
| 3. Results | 10 |
| 3.1. Hyperparameter Tuning | 10 |
| 3.2. Performance of the best Model | 10 |
| 4. Discussion | 16 |
| 4.1. Performance of the best Model | 16 |
| 5. Conclusion | 17 |
| 6. Acknowledgment and Declaration | 18 |
| 6.1. Acknowledgment | 18 |
| 6.2. Declaration of AI Usage | 18 |
| 6.3. Statement of Authorship | 19 |
| References | 20 |
| A. Appendix: Tables | 21 |

List of Figures

| | | |
|----|--|----|
| 1. | Visualization of the two transformations of the audio signal. | 8 |
| 2. | Flow chart illustrating the models architecture. N: elements in batch, C: channels, H: height, W: width, Cout: output channels, ks: kernel size, bc: base channels, nrb: number of residual blocks, n_classes: number of classes, nmp: parameter for max pooling | 9 |
| 3. | Accuracy of the models for different hyperparameter grouped by the transformation type. | 11 |
| 4. | Model size compared to the accuracy and F1 Score of the models. | 12 |
| 5. | F1 Score per class as mean trough all models compared to data distribution. | 13 |
| 6. | Available training data per classes compared to the F1 Score per classes in a scatter plot and the result of the Pearson correlation test. | 14 |
| 7. | Confusion matrix for the predictions of the test set using the best model. The over all accuracy on the test set was 0.649. | 15 |
| 8. | The validation loss and accuracy of the best model. Light version is not smoothed and dark version is smoothed with a window size of 5. | 16 |

List of Tables

| | | |
|----|--|----|
| 1. | Hyperparameters and values used for the grid search. | 7 |
| 2. | Results of the hyperparameter tuning by descending accuracy. | 21 |
| 3. | ClassID legend. | 22 |

1. Introduction

1.1. Background

One of the global environmental issues is the loss of biodiversity (Cardinale et al., 2012). The term biodiversity is a contraction of biological diversity, which refers to the variety and variability of life forms on Earth. In recent years, a massive decline in biodiversity has been observed, which is mainly due to human activities. The loss of biodiversity is a major concern because it can have a significant impact on the ecosystem and the services it provides (Brondízio et al., 2019). In order to quantify biodiversity and monitor its changes, it is essential to have a reliable and efficient method for quantifying biodiversity. Traditional methods for quantifying biodiversity are time-consuming and expensive, and they are not suitable for large-scale monitoring. But what if there was a non invasive method that could be used to monitor biodiversity in a fast and efficient way?

Bioacoustics, the study of sound production, dispersion and reception in animals, is an interesting field of research that focusses on the side of an individual species, group or community and their interaction with each other or their environment. It has provided amazing insights into the behavior and communication of animals. Ecoacoustics, a field of research very close to bioacoustics has a slightly different focus. It is the study of the soundscape of an ecosystem - the sounds produced by all living organisms in an ecosystem. The questions are typically a bit broader and about the composition of the soundscape, the temporal and spatial patterns of sound production, and the relationship between the soundscape and the environment. The study of biodiversity using bioacoustics is one of its promising applications even though there are still some issues to be fixed (Scarpelli et al., 2021). These passive acoustic monitoring (PAM) like the using of sound recordings to monitor biodiversity are currently widely researched and developed and even combined with modern artificial intelligence (AI) methods (Deng, 2023). Before there can be a holistic approach to the monitoring of biodiversity using ecoacoustics, some smaller steps have to be taken. One of these steps is the classification of the sounds of individual species or taxonomic groups. So far the taxonomic coverage includes birds, Cetaceans and other marine mammals, bats, terrestrial mammals, anurans, insects and fish (Stowell, 2022, p. 4). Birds are the most studied group of animals in the field of bioacoustics, with a commonly known and distributed application called the "BirdNET" (Kahl et al., 2021).

The focus of this study is to reproduce the results of the paper (Faiss, 2022) and to create a model that can classify a subset of insects using their voices. The subset contains members of the two groups of insects: *Orthoptera* and *Cicadidae*. *Orthoptera* is an order of insects that includes grasshoppers, crickets, and katydids. ("Orthoptera", 2008) *Cicadidae*, a members of the superfamily Cicadoidea Westwood are four-winged insects with sucking mouthparts that possess three ocelli and a rostrum that arises from the base of the head. (Sanborn, 2008) The goal is to proof that this technology is accessible for everyone with the knowledge and a regular gaming computer with a graphic processing unit (GPU). To achieve this, a model will be constructed and trained using the same dataset

as the original paper. A hyperparameter tuning will be performed to find the best configuration for the model. The results of the hyperparameter tuning will be evaluated and discussed. The best performing model will be tested and evaluated for its performance and accuracy. The results will be discussed and compared to the results of the original paper.

2. Methods

2.1. Dataset

In this study a preexisting dataset is used - the InsectSet32 dataset (Faiss, 2022). The dataset includes 335 recordings of 32 insect species, totaling 57 minutes. About half of the recordings (147) feature nine Orthoptera species from a dataset originally compiled by Baudewijn Odé (unpublished). The remaining 188 recordings, from 23 Cicadidae species, were selected from the Global Cicada Sound Collection on Bioacoustica (Baker et al., 2015a), including recordings published in (Baker et al., 2015b; Popple, 2017). Speech annotations at the beginning of many recordings led to using the last ten seconds of audio. Files with strong noise or multiple species were removed. The number of files per species ranges from four to 22, with durations from 40 seconds to almost nine minutes. All files, originally at least 44.1 kHz, were resampled to 44.1 kHz mono WAV for consistency. The dataset was already split into training, validation and test sets. There are two .csv files containing the labels and the filenames of the recordings.

2.2. Programming Language and Frameworks

To build and train the deep learning model, the programming language Python was used. The Frameworks PyTorch, Lightning are very popular and powerful tools for building deep learning models.

2.3. Deep Learning Model

The deep learning model used in this study is a convolutional neural network (CNN) with residual blocks illustrated in Figure 2. It consists of three main parts: An input layer, a number of residual blocks and an fully connected output layer. The input layer is a convolutional layer with a kernel size of 1 and output channels set to the base channels (bc) - for this experiment it was set to 8. After the convolutional layer, the input is normed with a batch normalization layer and then passed through a ReLU activation function. This output is then passed through a number of residual blocks. The model is implemented dynamically, so the number of residual blocks can be set as a hyperparameter. Each residual block consists of two convolutional layers, each followed by a batch normalization layer and a ReLU activation function. The output channels are doubled with every residual block. The residual connection is implemented by passing the input through a separated convolutional layer with a kernel size of 1 and the same number of output channels as the output of the convolutional layers in the residual block to match dimensions. This output is then added to the output of the transformation in the residual block. At the end of the residual block, the output is passed through a max pooling layer to reduce the dimensions. The max pooling layer is implemented to alter the kernel size with every residual block. For every odd residual block the kernel size is set to `n_max_pool` - in this experiment it

was set to 3 - reducing the dimensions by a factor of 3. For every even residual block the kernel size is set to 1, so the dimensions stay the same. The output of the residual blocks is then passed through a fully connected layer, consisting of a global average pooling layer to reduce the dimensions to the number of classes. An additional convolutional layer with kernel size 1 to match the number of classes. A flattening layer to get of the dimensions H and W already reduced to 1 and a softmax activation function to get the probabilities for each class as a vector of length n_classes - in this experiment 32 - elements between 0 and 1 that sum up to 1.

2.4. Data Processing

A custom Dataloader was implemented, to handle the data processing on the fly and provide the trainer with then data samples matching the chosen indices. To implement the dataloader, the PyTorch Dataset and DataLoader classes where used. For the data processing, the torchaudio and numpy libraries where used. There is two steps to the data processing: Sampling and Transformation.

2.4.1. Sampling

The audio files are of different lengths and the model can only handle inputs of a fixed size. Since the smallest files are of a length of around 1 second and the longest file is around 160 seconds, a compromise had to be made. To only sample the files to a length of 1 second would mean very little information being available for the model to learn from. On the other hand if the files are sampled for a length of more than a second, the short files would need to be padded with zeros meaning the file starts with a basically empty part. This could lead to the model learning from the length of the empty part and not the actual audio signal. To avoid this, the audio files where sampled to a random length between 1 and 10 seconds and then padded with zeros to the fixed length of 10 seconds. To implement this, a custom method was implemented as shown in Listing 1.

Listing 1: Python code for the sampling of the filies

```
1 import numpy as np
2 import torch
3
4 def get_random_part_padded(self, waveform: Tensor, samplerate: int) -> Tensor:
5
6     min_len_in_samples = int(self.min_len_in_seconds * samplerate)
7     max_len_in_samples = int(self.max_len_in_seconds * samplerate)
8
9     if self.min_len_in_seconds == -1:
10         sample_start_index = -max_len_in_samples
11         sample_end_index = None
12
13     else:
14         part_length = np.random.randint(min_len_in_samples, max_len_in_samples +
15                                         1)
16         sample_length = waveform.shape[1]
17         part_length = min(part_length, sample_length)
```

```

17     sample_start_index = np.random.randint(0, sample_length - part_length +
18     1)
19     sample_end_index = sample_start_index + part_length
20
21     waveform_part = waveform[:, sample_start_index:sample_end_index]
22     actual_part_length = waveform_part.shape[1]
23     pad_length = max_len_in_samples - actual_part_length
24     waveform_pad = torch.nn.functional.pad(waveform_part, pad=(pad_length, 0, 0,
25     0))
26
27     return waveform_pad

```

2.4.2. Transformation

The model is actually one, usually used for image classification and therefore expects two dimensional input while an audio file has only one dimension. To transform the samples into into a format, that the model can handle, a short time Fourier transformation (STFT) was applied. The Fourier transformation is a mathematical operation that transforms a function of time into a function of frequency. An other way to describe this is, that a series of spectrograms for short time slices of the audio signal are created and aligned in a 2D array - basically a visualization of the audio signal and therefore something a image classification model can handle. In addition a second version was implemented, where the STFT where transformed additionally. The two versions are visualized for a random sample with no padding in Figure 1. The frequency bins were transformed into mel bins, which are a more human like representation of the frequency content of the audio signal. This transformation is called a mel-spectrogram and is commonly used in the field of ecoacoustics (Stowell, 2022, p. 7). Both versions of the transformation where transformed into decibels and normalized before being passed into the model.

To implement the two varieties of the transformation, the library torch and torchaudio where used. A custom transformation method was implemented, that can be used as a layer in the model as shown in Listing 2. Some of the parameters of the transformation where made configurable and others dependant on them where calculated. In the hyperparameter tuning phase, the only parameter that was tuned was the number of mel bins, which was set to either 64 to try the mel-spectrogram or -1 to use the standard spectrogram.

Listing 2: Python code for the transformation of the audio signal

```

1  import torch
2  import torchaudio
3
4  class NormalizeSpectrogram(torch.nn.Module):
5      def forward(self, tensor):
6          return (tensor - tensor.min()) / (tensor.max() - tensor.min())
7
8  normalize_transform = NormalizeSpectrogram()
9
10 if n_mels == -1:
11     spectrogram = torchaudio.transforms.Spectrogram(
12         n_fft=n_fft,
13         hop_length=int(n_fft/2),
14         win_length=n_fft)

```

```

15 else:
16     spectrogram = torchaudio.transforms.MelSpectrogram(
17         n_fft=n_fft,
18         hop_length=int(n_fft/2),
19         win_length=n_fft,
20         n_mels=n_mels,
21         f_max=self.sample_rate / 2)
22
23 db_transform = torchaudio.transforms.AmplitudeToDB(top_db=top_db)
24
25 self.transform = torch.nn.Sequential(
26     spectrogram,
27     db_transform,
28     normalize_transform)

```

2.5. Fitting the Model

The training was completely handled by the PyTorch Lightning framework. The logging was done with the TensorBoard logger and with an additional custom logger to get easier access to the data afterwards. The hyperparameter grid search was implemented with a custom Python script.

2.5.1. Training

The training was done on a single GPU. The model was trained for a maximum of 2000 epochs with a early stopping callback, that stopped the training if the validation loss did not improve for patience = 100 epochs. The model was trained with a batch size of 10. The optimizer used was the AdamW optimizer of the PyTorch library with a weight decay of 0. The loss function used was the CrossEntropyLoss function of the PyTorch library with default parameters and class weights according to available data per class. Different learning rates were tried during the hyperparameter tuning referred to in Section 2.5.2. Only the best model was saved and used for the evaluation of the model. In order to simplify the evaluation, on completion of the training the whole dataset was predicted and saved to a csv file in the log folder.

2.5.2. Hyperparameter Tuning

For the hyperparameter tuning, a select number of hyperparameters were chosen to be tuned. Considerations like the experience of some early tests, the computational resources available and the time frame of the project were taken into account. The hyperparameters that were chosen for the grid search are shown in Table 1. For the grid search, models for all possible combinations of the hyperparameters - in this case $2 \times 3 \times 2 \times 3 = 36$ were trained. To implement the grid search a short Python script was written to create the system commands to start the training with the different hyperparameter combinations.

Table 1: Hyperparameters and values used for the grid search.

| Hyperparameter | Description | Variations | Values |
|----------------|--------------------------------------|------------|---------------|
| n_mels | transformation (-1 for regular STFT) | 2 | 64, -1 |
| n_res_blocks | number of res blocks | 3 | 2, 3, 4 |
| learning_rate | step size during optimization | 2 | 0.001, 0.0001 |
| kernel_size | dimension of the filter | 3 | 3, 5, 7 |

2.6. Evaluation

To evaluate the models, the predictions already implemented at the end of the training. The output of the model was a vector of length 32 with probabilities for each class, they were transformed into a predicted class ID by taking the index of the highest probability using the argmax function of the numpy library. For all the models they were stored in a csv file in their log folder. To evaluate the hyperparameter tuning the predictions of the validation set were used, as they were not used during the training of the model except for the early stopping and the selection of the best model. To evaluate the best model, only the predictions of the test set were used.

2.6.1. Metrics and Tests

Accuracy: The accuracy is the ratio of correctly predicted observations to the total observations. It was calculated using the mean function of the numpy library:

`np.mean(y_true == y_pred)` The accuracy was the metric chosen to choose the best model for further evaluation.

F1 Score: The F1 score is a metric that combines the precision and recall of a model. In this case the macro average was used, which calculates the F1 score for each class and then takes the mean. It was calculated using the `f1_score` function of the sklearn library:

`f1_score(y_true, y_pred, average='macro', sample_weight=None, zero_division='warn')`

F1 Score per Class: The F1 score per class is the F1 score for each class. It was calculated using the `f1_score` function of the sklearn library with the average parameter set to None:

`f1_score(y_true, y_pred, average=None, sample_weight=None, zero_division='warn')`

It was calculated for each class and for each model from the hyperparameter tuning. The results were then aggregated to get the mean F1 score per class over all models. The results were then visualized in a bar chart combined with the available data per class - refer to figure 5.

Confusion Matrix: The result of the Predictions of the best model were used to create a confusion matrix. The confusion matrix is a table that is often used to analyze the performance of a classification model. Predictions and true labels are compared and

visualized in a matrix shown in figure 7. The confusion matrix in Figure was calculated using the `confusion_matrix` function of the `sklearn` library.

Pearson Test: The Pearson test was used to test the correlation between the model size and the accuracy or F1 score of the models. The Pearson test was calculated using the `pearsonr` function of the `scipy` library:

```
for i, metric in enumerate(['accuracy', 'f1']):  
    pearson_corr, p_value = stats.pearsonr(ex.summary[metric], ex.summary['num_trainable_params'])
```

And the correlation between the train data count and the F1 score per class:

```
pearson_corr, p_value = stats.pearsonr(data['f1'], data['count'])
```

For both cases the null hypothesis (H_0) posited that there is no correlation, with the significance level (α) set at 0.05.

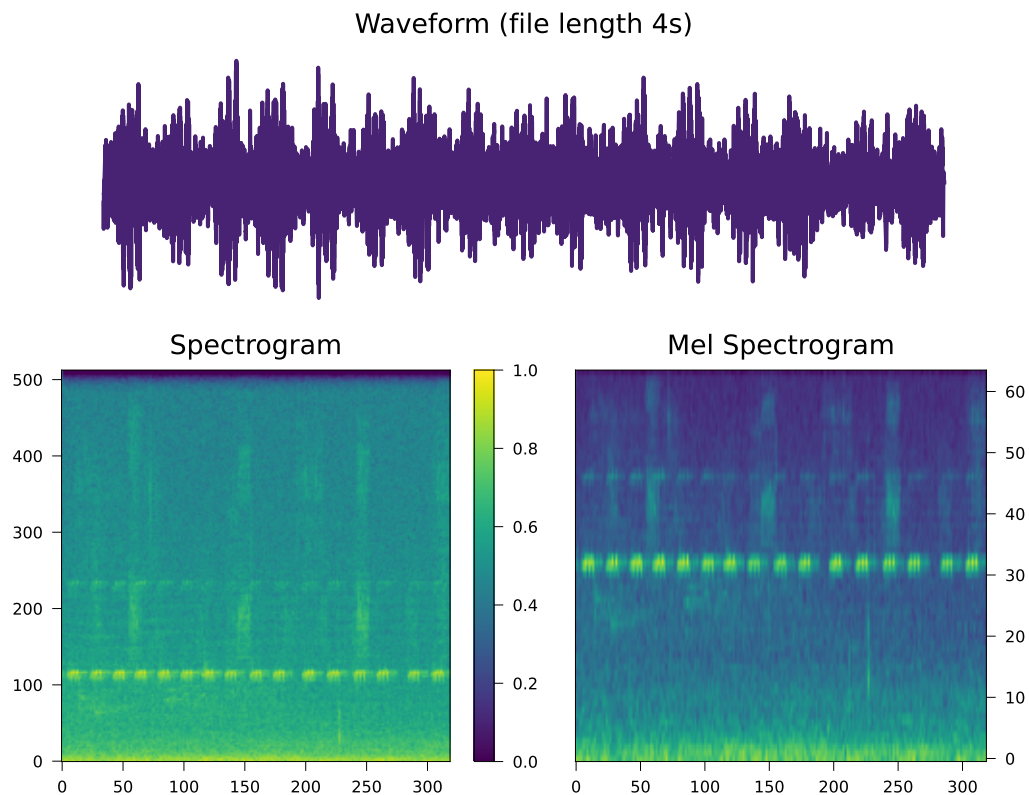
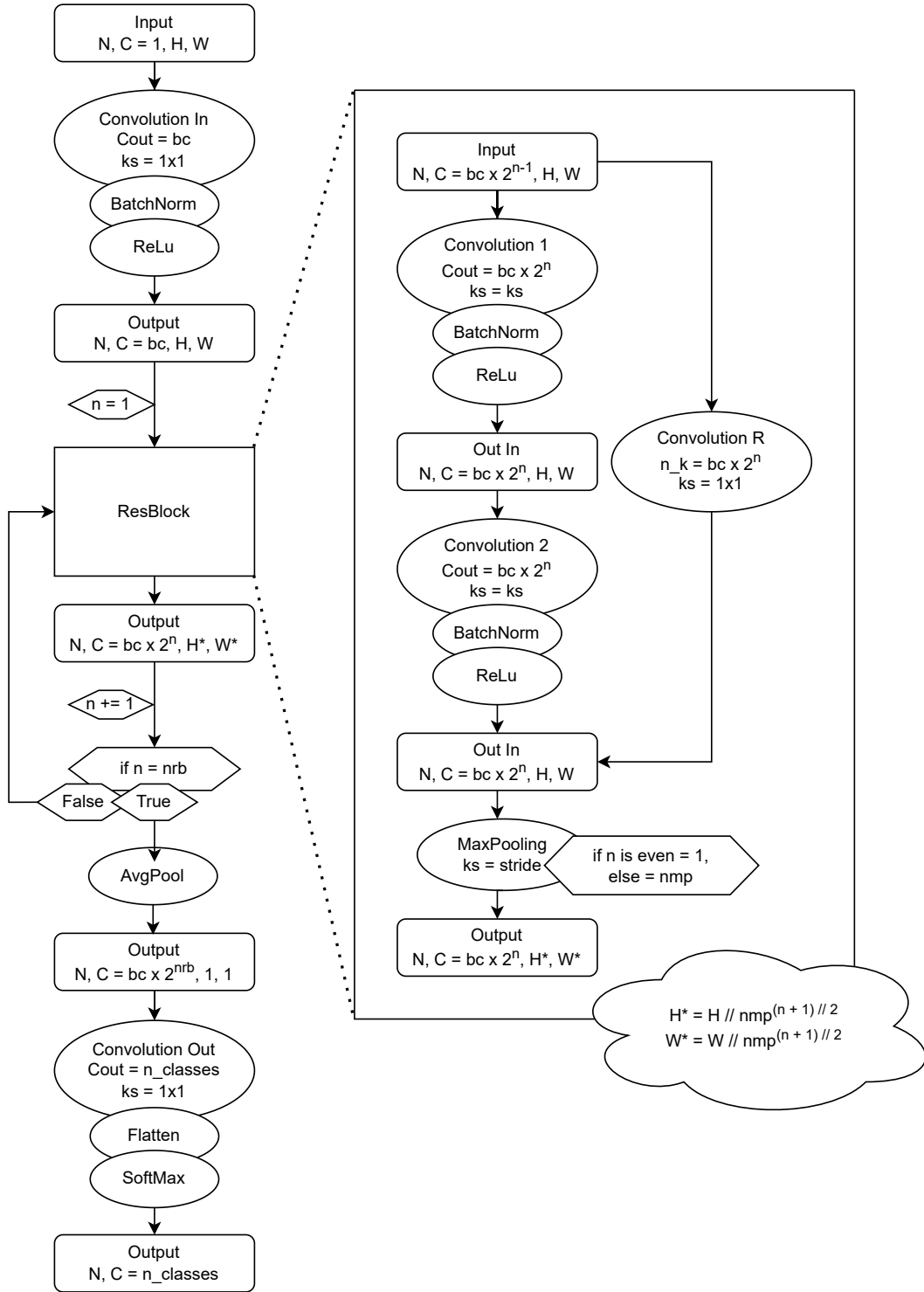


Figure 1: Visualization of the two transformations of the audio signal.



3. Results

3.1. Hyperparameter Tuning

The detailed results of the Hyperparameter tuning are shown in table 2. The ranking of the score according to the accuracy or the F1 score are similar but there are some differences. As an example is the best performance according to the accuracy 0.706 with an F1 score of 0.571 while the best score according to the F1 score is 0.608 with an accuracy of 0.667 - so the best model differs in the two scores. It is quite difficult to find any obvious tendencies for the influence of the hyperparameters on the performance of the model. Figure 3 shows the distribution of the accuracy comparing different different hyperparameters grouped by the transformation used. There is a tendency visible for the MelSpectrogram to work a bit better. A smaller learning rate seems to deliver results a bit less distributed but the difference is not very big. For the MelSpectrogram transformation the number of ResBlocks seems to have a bigger influence on the performance - two seems not to be enough. Furthermore there is a tendency for smaller kernel sizes to deliver less distributed results but a better performance is achieved with a kernel size of 5. In figure 4 the models size measured by the number of trainable parameters is plotted against the accuracy and the F1 score. There is no obvious correlation visible between the model size and the performance of the model. This is also supported by the results of the Pearson Test. For both metrics the p value is far above 0.05 leaving the null hypothesis that there is no significant correlation between the model size and the performance of the model. The r values both quite close to zero but negative indicate that there might be a slight tendency for a smaller model to perform better. The F1 score per class is shown in figure 5 and compared to the distribution of the available data. Class 11 has a very low F1 score compared to the available data while class 9 has a very high F1 Score compared to the available data. To further examine the relation between the F1 score and the distribution of the data in figure 6 the F1 score is plotted against the distribution of the training data. There is no obvious correlation visible between the F1 score and the distribution of the data. This is also supported by the results of the Pearson Test. The p value is above 0.05 leaving the null hypothesis that there is no significant correlation. The r value is positive therefore there might be a slight tendency for more training data to deliver a better F1 score.

3.2. Performance of the best Model

The best performing configuration for the model was found to be the one with the following hyperparameters:

- **n_mels:** 64
- **n_res_blocks:** 4
- **learning_rate:** 0.001
- **kernel_size:** 5

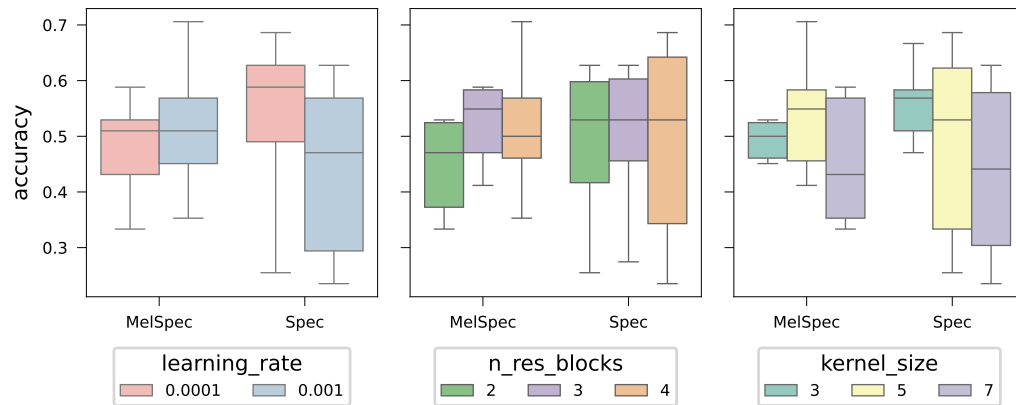
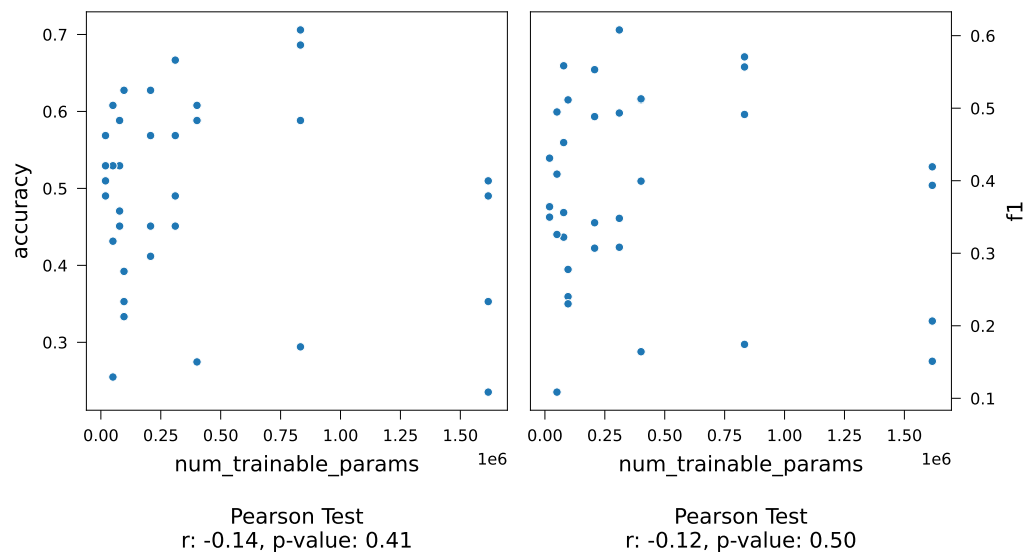


Figure 3: Accuracy of the models for different hyperparameter grouped by the transformation type.

On the test set, the model achieved an accuracy of 0.649 and an F1 score of 0.546. The confusion matrix for the predictions generated by this model is shown in Figure 7. The concentration of results in the diagonal of the confusion matrix indicates that the model is performing well. Class 22 was predicted the most frequent with more than 50% of the predictions being wrong.



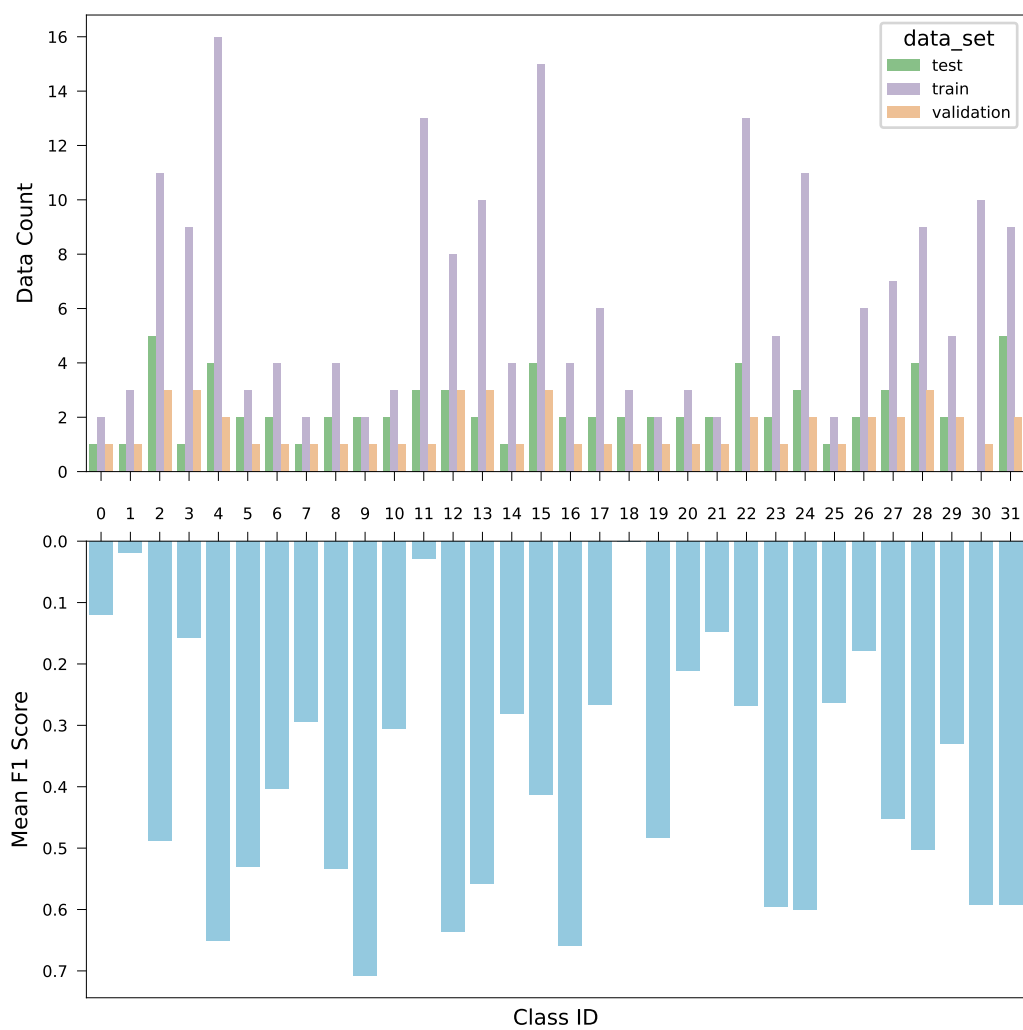


Figure 5: F1 Score per class as mean trough all models compared to data distribution.

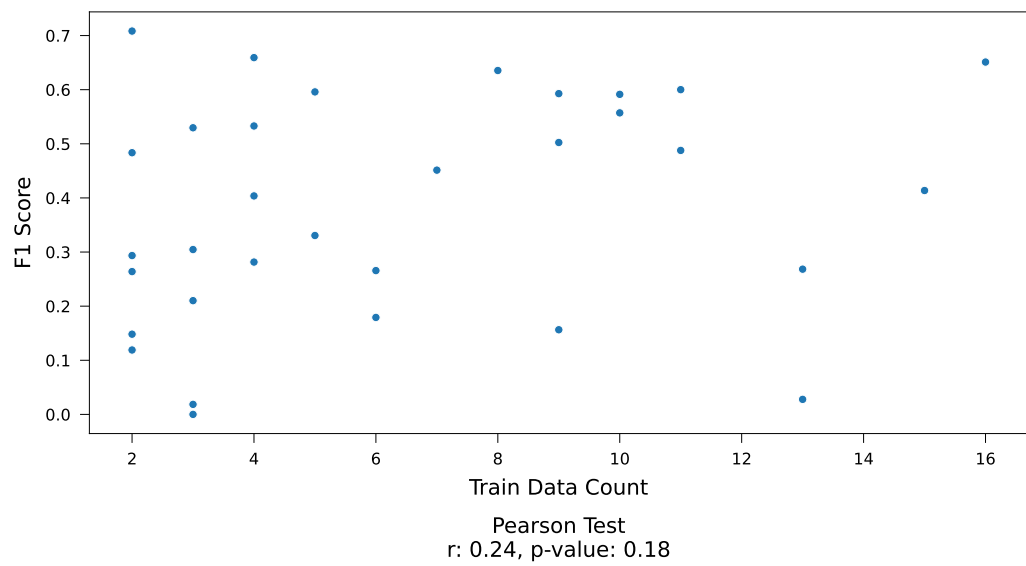


Figure 6: Available training data per classes compared to the F1 Score per classes in a scatter plot and the result of the Pearson correlation test.

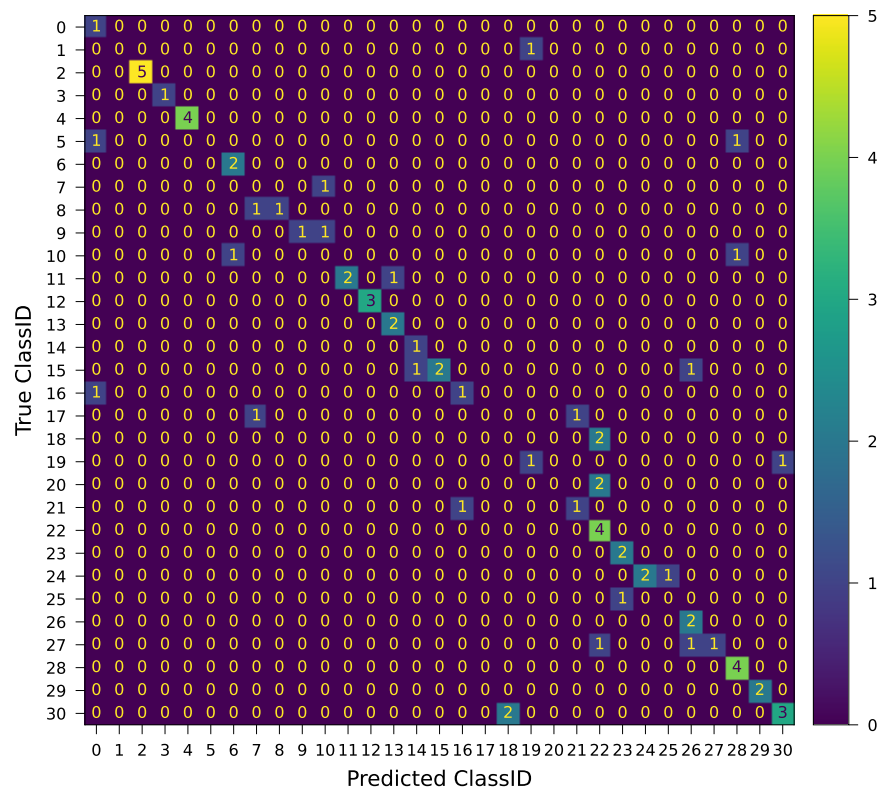


Figure 7: Confusion matrix for the predictions of the test set using the best model. The over all accuracy on the test set was 0.649.

4. Discussion

4.1. Performance of the best Model

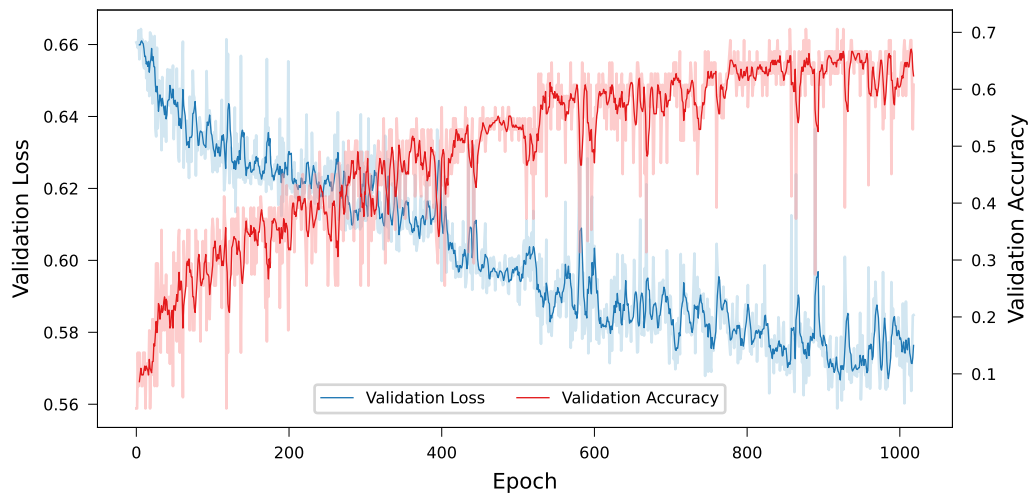


Figure 8: The validation loss and accuracy of the best model. Light version is not smoothed and dark version is smoothed with a window size of 5.

5. Conclusion

6. Acknowledgment and Declaration

6.1. Acknowledgment

I would like to express my gratitude to my brother, Dr. Basil Kraft for his continuous support and expertise in the field of machine learning. Without his help, this project would not have been possible.

6.2. Declaration of AI Usage

GitHub Copilot was used to assist writing the code and text for this project.

ChatGPT was used to assist researching, writing the code and text for this project.

N-FO-Formular Statement of Authorship for
Student Work



**Life Sciences und
Facility Management**

Education Unit

Statement of Authorship for Student Work at the School of Life Sciences and Facility Management

By submitting the enclosed

- ☐ Project
- ☐ Literature review
- ☐ Course work
- ☒ Minor paper
- ☐ Bachelor's thesis
- ☐ Master's thesis (tick as appropriate)

the student affirms independent completion of the(ir) work without outside help.

The undersigned student declares that all printed and electronic sources used in the text and the bibliography are correctly indicated, i.e., that the work does not contain any plagiarism (no parts that have been taken in whole or in part from another's or his/her own text or from another's or his/her own work without clear identification and without stating the source).

In the event of misconduct of any kind, Paragraph 39 and Paragraph 40 of the General Academic Regulations for Bachelor's and Master's degree programmes at the Zurich University of Applied Sciences (dated 29 January 2008) and the provisions of the Disciplinary Measures of the University Regulations shall apply.

Location, date:

Student signature:

Neuhausen, 2024-6-27

Note on submitting the Statement of Authorship:

Direct submission of the work: This Statement of Authorship is to be inserted in the appendix of the ZHAW version of all work with original signatures and date (copies will not be accepted).

Submission of the work via Compliesis: The Statement of Authorship should be made directly in Compliesis by clicking as directed and should not be inserted in the appendix of the work.

| | | | |
|--------------------------|-------------------------------|-----------------|-----------------------|
| Erlassverantwortliche/-r | LeiterIn Stabsbereich Bildung | Ablageort | 2.05.00 Lehre Studium |
| Beschlussinstanz | LeiterIn Stab | Publikationsort | Public |
| Genehmigungsinstanz | | | |

| Version | Beschluss | Beschlussinstanz | Inkrafttreten | Beschreibung Änderung |
|---------|------------|------------------|---------------|---|
| 1.0.0 | 15.03.2022 | LeiterIn Stab | 15.03.2022 | Originalversion |
| 1.1.0 | 15.04.2024 | Leiter:in Stab | 01.5.2024 | Adding clarification on self-plagiarism |

References

- Cardinale, B. J., Duffy, J. E., Gonzalez, A., Hooper, D. U., Perrings, C., Venail, P., Narwani, A., Mace, G. M., Tilman, D., Wardle, D. A., Kinzig, A. P., Daily, G. C., Loreau, M., Grace, J. B., Larigauderie, A., Srivastava, D. S., & Naeem, S. (2012). Biodiversity loss and its impact on humanity. *Nature*, 486(7401), 59–67. <https://doi.org/10.1038/nature11148>
- Brondízio, E. S., Settele, J., Díaz, S., & Ngo, H. T. (Eds.). (2019). *The global assessment report of the intergovernmental science-policy platform on biodiversity and ecosystem services*. Intergovernmental Science-Policy Platform on Biodiversity and Ecosystem Services (IPBES). OCLC: 1336011247.
- Scarpelli, M. D. A., Lique, B., Tucker, D., Fuller, S., & Roe, P. (2021). Multi-Index Ecoacoustics Analysis for Terrestrial Soundscapes: A New Semi-Automated Approach Using Time-Series Motif Discovery and Random Forest Classification. *Frontiers in Ecology and Evolution*, 9, 738537. <https://doi.org/10.3389/fevo.2021.738537>
- Deng, I. (2023). Harnessing the Power of Sound and AI to track Global Biodiversity Framework (GBF) Targets.
- Stowell, D. (2022). Computational bioacoustics with deep learning: A review and roadmap. *PeerJ*, 10, e13152. <https://doi.org/10.7717/peerj.13152>
- Kahl, S., Wood, C., Eibl, M., & Klinck, H. (2021). BirdNET: A deep learning solution for avian diversity monitoring. *Ecological Informatics*, 61, 101236. <https://doi.org/10.1016/j.ecoinf.2021.101236>
- Faiss, M. (2022, September 12). *InsectSet32: Dataset for automatic acoustic identification of insects (Orthoptera and Cicadidae)* (Version 0.1). Zenodo. <https://doi.org/10.5281/zenodo.7072196>
- Orthoptera. (2008). In J. L. Capinera (Ed.), *Encyclopedia of Entomology* (pp. 2695–2695). Springer Netherlands. https://doi.org/10.1007/978-1-4020-6359-6_1892
- Sanborn, A. (2008). Cicadas (Hemiptera: Cicadoidea). In J. L. Capinera (Ed.), *Encyclopedia of Entomology* (pp. 874–877). Springer Netherlands. https://doi.org/10.1007/978-1-4020-6359-6_666
- Baker, E., Price, B., Rycroft, S., Hill, J., & Smith, V. S. (2015a). BioAcoustica: A free and open repository and analysis platform for bioacoustics. *Database*, 2015, bav054. <https://doi.org/10.1093/database/bav054>
- Baker, E., Price, B., Rycroft, S., & Villet, M. (2015b). Global Cicada Sound Collection I: Recordings from South Africa and Malawi by B. W. Price & M. H. Villet and harvesting of BioAcoustica data by GBIF. *Biodiversity Data Journal*, 3, e5792. <https://doi.org/10.3897/BDJ.3.e5792>
- Popple, L. W. (2017). A revision of the *Myopsalta crucifera* (Ashton) species group (Hemiptera: Cicadidae: Cicadettini) with 14 new species from mainland Australia. *Zootaxa*. <https://doi.org/10.11646/zootaxa.4340.1>

A. Appendix: Tables

Table 2: Results of the hyperparameter tuning by descending accuracy.

| n_mels | res blocks | learning rate | kernel size | parameters | epochs | accuracy | F1 |
|--------|------------|---------------|-------------|------------|--------|----------|-------|
| 64 | 4 | 0.001 | 5 | 832,912 | 1018 | 0.706 | 0.571 |
| -1 | 4 | 0.0001 | 5 | 832,912 | 672 | 0.686 | 0.557 |
| -1 | 4 | 0.0001 | 3 | 310,544 | 891 | 0.667 | 0.608 |
| -1 | 3 | 0.001 | 5 | 207,376 | 394 | 0.627 | 0.553 |
| -1 | 2 | 0.0001 | 7 | 96,528 | 1198 | 0.627 | 0.511 |
| -1 | 2 | 0.001 | 5 | 50,256 | 640 | 0.608 | 0.495 |
| -1 | 3 | 0.0001 | 7 | 401,104 | 760 | 0.608 | 0.512 |
| -1 | 3 | 0.0001 | 3 | 78,224 | 897 | 0.588 | 0.558 |
| 64 | 4 | 0.0001 | 5 | 832,912 | 371 | 0.588 | 0.491 |
| 64 | 3 | 0.0001 | 7 | 401,104 | 536 | 0.588 | 0.513 |
| 64 | 3 | 0.001 | 7 | 401,104 | 350 | 0.588 | 0.399 |
| 64 | 3 | 0.001 | 5 | 207,376 | 505 | 0.569 | 0.488 |
| -1 | 2 | 0.001 | 3 | 19,408 | 469 | 0.569 | 0.431 |
| -1 | 4 | 0.001 | 3 | 310,544 | 562 | 0.569 | 0.493 |
| 64 | 3 | 0.0001 | 3 | 78,224 | 1115 | 0.529 | 0.453 |
| 64 | 2 | 0.001 | 5 | 50,256 | 661 | 0.529 | 0.409 |
| 64 | 2 | 0.0001 | 3 | 19,408 | 1354 | 0.529 | 0.365 |
| 64 | 4 | 0.0001 | 7 | 1,616,464 | 273 | 0.510 | 0.419 |
| 64 | 2 | 0.001 | 3 | 19,408 | 455 | 0.510 | 0.364 |
| -1 | 4 | 0.0001 | 7 | 1,616,464 | 296 | 0.490 | 0.394 |
| -1 | 2 | 0.0001 | 3 | 19,408 | 1138 | 0.490 | 0.350 |
| 64 | 4 | 0.001 | 3 | 310,544 | 408 | 0.490 | 0.348 |
| -1 | 3 | 0.001 | 3 | 78,224 | 456 | 0.471 | 0.356 |
| -1 | 3 | 0.0001 | 5 | 207,376 | 531 | 0.451 | 0.342 |
| 64 | 4 | 0.0001 | 3 | 310,544 | 330 | 0.451 | 0.308 |
| 64 | 3 | 0.001 | 3 | 78,224 | 474 | 0.451 | 0.322 |
| 64 | 2 | 0.0001 | 5 | 50,256 | 892 | 0.431 | 0.326 |
| 64 | 3 | 0.0001 | 5 | 207,376 | 395 | 0.412 | 0.307 |
| -1 | 2 | 0.001 | 7 | 96,528 | 375 | 0.392 | 0.240 |
| 64 | 4 | 0.001 | 7 | 1,616,464 | 403 | 0.353 | 0.207 |
| 64 | 2 | 0.001 | 7 | 96,528 | 229 | 0.353 | 0.230 |
| 64 | 2 | 0.0001 | 7 | 96,528 | 545 | 0.333 | 0.278 |
| -1 | 4 | 0.001 | 5 | 832,912 | 290 | 0.294 | 0.174 |
| -1 | 3 | 0.001 | 7 | 401,104 | 268 | 0.275 | 0.164 |
| -1 | 2 | 0.0001 | 5 | 50,256 | 432 | 0.255 | 0.109 |
| -1 | 4 | 0.001 | 7 | 1,616,464 | 145 | 0.235 | 0.151 |

Table 3: ClassID legend.

| ClassID | Species | ClassID | Species |
|---------|--------------------------|---------|-----------------------------|
| 0 | Azanicadazuluensis | 16 | Platyleurachalybaea |
| 1 | Brevisianabrevis | 17 | Platyleuradeusta |
| 2 | Chorthippusbiguttulus | 18 | Platyleuradivisa |
| 3 | Chorthippusbrunneus | 19 | Platyleurahaglundii |
| 4 | Grylluscampestris | 20 | Platyleurahirtipennis |
| 5 | Kikihiamuta | 21 | Platyleuraintercapedinis |
| 6 | Myopsaltaleona | 22 | Platyleuraplumosa |
| 7 | Myopsaltalongicauda | 23 | Platyleurasp04 |
| 8 | Myopsaltamackinlayi | 24 | Platyleurasp10 |
| 9 | Myopsaltamelanobasis | 25 | Platyleurasp11cfhirtipennis |
| 10 | Myopsaltaxerograsidia | 26 | Platyleurasp12cfhirtipennis |
| 11 | Nemobiussylvestris | 27 | Platyleurasp13 |
| 12 | Oecanthuspellucens | 28 | Pseudochorthippusparallelus |
| 13 | Pholidopteragriseoaptera | 29 | Pycnasemiclara |
| 14 | Platyleuracapensis | 30 | Roeselianaroeselii |
| 15 | Platyleuracfcatenata | 31 | Tettigoniaviridissima |